Astron. Astrophys. 345, 943–948 (1999)

ASTRONOMY AND ASTROPHYSICS

The structure and dynamics of the unique Honeycomb Nebula in the halo of 30 Doradus

M.P. Redman[1], **Z.A. Al-Mostafa**[1,2], **J. Meaburn**[1], **M. Bryce**[1], **and J.E. Dyson**[3]

[1] Department of Physics and Astronomy, University of Manchester, Oxford Road, Manchester M13 9PL, UK
[2] King Abdulaziz City for Science and Technology, Institute of Astronomical and Geophysical Research, P.O. Box 6086, Riyadh 11442, Saudi Arabia
[3] Department of Physics and Astronomy, University of Leeds, Leeds, LS2 9JT, UK

Received 3 November 1998 / Accepted 2 March 1999

Abstract. The structure and dynamics of the Honeycomb nebula in the Large Magellanic cloud are modelled as resulting from the interaction of a supernova explosion with an existing giant shell of the type commonly found in the LMC. In particular, the processes that may have led to the striking morphology and velocity structure of this nebula are examined. New data of the Honeycomb nebula, are presented. Here, spatially resolved profiles of the [S II] 6716 & 6731 Å density sensitive lines, obtained with the Manchester Echelle Spectrometer, supplement previous, complementary, Hα and [N II] 6584 Å profiles.

The agreements and differences between all of these data and this simple model are highlighted.

Key words: ISM: kinematics and dynamics – ISM: supernova remnants – ISM: magnetic fields – galaxies: Magellanic Clouds

1. Introduction

The unusual morphology and kinematics of the Honeycomb nebula in the Large Magellanic Cloud (LMC) has led to considerable interest in the processes that led to its formation. Images of the Honeycomb nebula, discovered by Wang (1992), are presented in Fig. 1a,b.

Meaburn et al. (1993) considered several possible explanations for the origin of the Honeycomb. These were all found to be improbable and included individual wind blown bubbles or supernova shells and mass-loaded flows past large clumps. Meaburn et al. (1993), Chu et al. (1995) and Meaburn et al. (1995) all favoured the collision of a supernova blast wave with pre-existing, clumpy, dense gas. Chu et al. (1995) used a combination of archival x-ray and radio data with their CCD images to demonstrate convincingly the supernova remnant nature of the Honeycomb. It exhibits the three classical supernova remnant signatures. These are bright X-ray emission, non-thermal synchrotron emission and enhanced $[\mathrm{Sii}]/\mathrm{H}\alpha$ ratios. Of particular interest is the fact that the radio spectrum is steep - a common feature of young supernova remnants.

Send offprint requests to: M.P. Redman (mpr@ast.man.ac.uk)

The supernova explosion itself presumably took place within a rarefied cavity of hot gas rendering the remnant invisible in optical images (the so-called 'muffling' effect). Only in those portions of the blast wave encountering a significant obstacle to their progress can the shock speed drop enough for optical emission to occur. The obstacle is most likely to be either the inside of a giant (100 pc diam.) pre-existing shell (Meaburn et al. 1993) or a more localised intervening sheet of dense gas (Chu et al. 1995). There is supporting evidence for both of these possibilities. Meaburn et al. (1995) find faint, extended, redshifted emission associated with the Honeycomb that may be compared to the prominent and dramatic blueshifted velocity spikes found at the edges of the Honeycomb's component cells. The redshifted emission was interpreted as emission from the far wall of the giant shell (the blue shifted spikes indicate that gas was shocked from behind and is thus the near wall of the shell). If this giant shell were complete, however, then the honeycomb structure should be more extensive than it is, which might favour the Chu et al. (1995) porous sheet of dense gas interpretation.

The Honeycomb nebula resides in the outer regions of the highly active 30 Doradus complex. From both kinematical and morphological observations it became clear (Meaburn 1988, 1991) that 30 Doradus consists of interlocking giant shells, surrounding hollow cavities, expanding at $\approx 35\mathrm{km\,s^{-1}}$. They are tens of parsec in diameter in the dense, young (Walborn et al. 1999) core of the complex but reach 100 pc diameter at its lower density periphery which is populated by older stars. These outer giant shells are most likely in a momentum conserving phase (similar to N11 - see Meaburn et al. 1989) and have each been formed by successive supernova explosions and stellar winds of the enclosed older OB associations. There is much kinematical evidence for recent supernova activity ($\approx$ 40 explosions within 10^4 yr) in the halo of 30 Doradus alone (Meaburn 1991), the latest being SN 1987a.

The Honeycomb nebula has therefore been formed within a system of interlocked shells and giant shells which, since they are not formed in isolation, could each be significantly disrupted. In this paper it is assumed that the Honeycomb nebula is generated by the blast wave of a recent supernova explosion, inter-

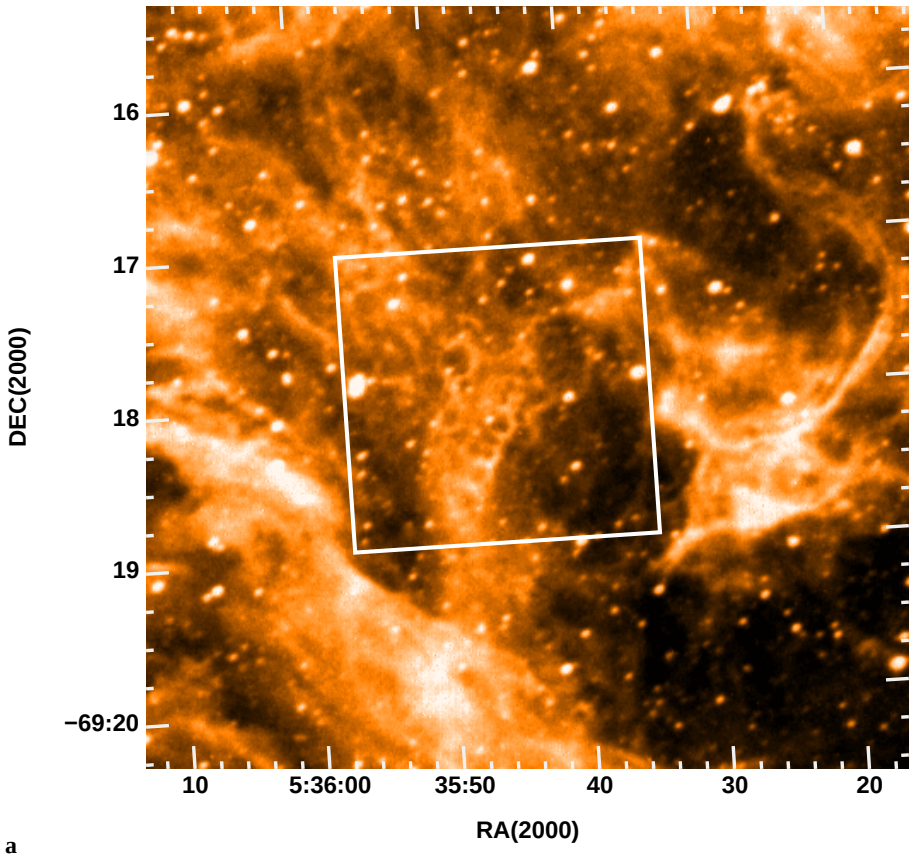

a

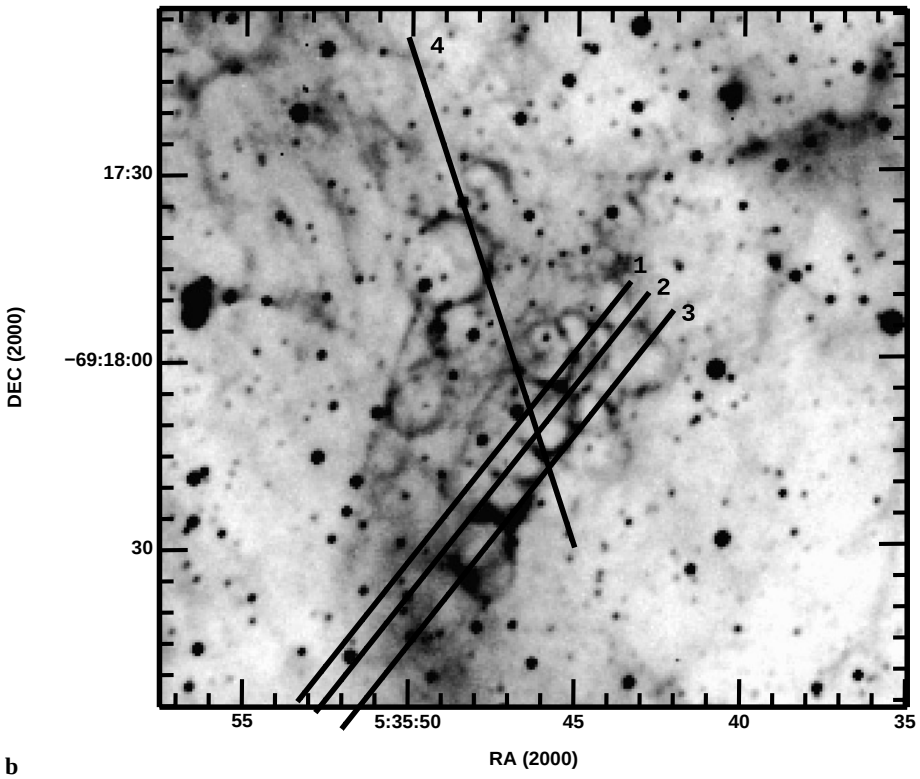

b

Fig. 1. **a** An Hα + [N II] 6584 Å image of the environment of the Honeycomb nebula is shown. This is taken from a UK Schmidt image scanned by SuperCosmos. **b** An NTT (Wang 1992) Hα + [N II] 6584 Å image of the Honeycomb nebula from the area marked by the white box in **a**.

acting with a nearby large fragment of a pre-existing giant shell at the periphery of the 30 Doradus region.

Although from the discussion above, the origin of the Honeycomb nebula seems reasonably clear, the generation of the

intriguing structure and kinematics is far less so and is the main subject of this paper. In Sect. 2 new kinematical and density data, obtained with the Manchester echelle spectrometer, is presented. Shells driven by multiple supernovae are reviewed in Sect. 3. The Honeycomb nebula is modelled in Sect. 4 and the results are compared with the observations. Conclusions are drawn in Sect. 5.

2. Observations

The spatially resolved, longslit observations of the profiles of the [S II] 6716 & 6731 Å lines were made using the dedicated Manchester echelle spectrometer (MES – Meaburn et al. 1984) in combination with the 3.9m Anglo-Australian Telescope and a Tek 1024x1024 CCD detector. On the nights of 1994 October 13–20 in which these profiles were obtained, the 'seeing' remained stable at a remarkable 0.8″. A slit length equivalent to 163″ and slit width of $150\,\mu$m ($\equiv 10$km s^{-1} and 1″) were employed. All spectral observations were calibrated to $\pm\,1\mathrm{km\,s^{-1}}$ accuracy against the spectrum of a Th/Ar emission line lamp. The echelle order containing the [S II] 6716 & 6731 Å emission lines was isolated using an interference filter of 90 Åbandwidth.

Parts of the slit lengths for positions 1–4 where the [S II] 6716 & 6731 Å profiles were obtained are marked against the Hα + [N II] 6584 Å image of the Honeycomb nebula in Fig. 1b which is shown relative to the filaments of the halo of 30 Dor in Fig. 1a.

Negative, greyscale representations of the [S II] 6731 Å line profiles along Slits 1–4 are shown in Figs. 2a–d respectively. These should be compared with the complementary Hα profiles in Meaburn et al. (1993,1995).

The measurements of the local electron densities, $N_{\rm e}$, for $T_{\rm e} = 10^4$ K for different velocity features marked A–H in Figs. 2a,b are tabulated in Table 1. The densities in the velocity spikes are marked A–F and in the ambient medium, G–H. The collision strengths of Saraph & Seaton (1979) were used the convert the measured [S II] 6716 Å/6731 Å brightness ratios into these $N_{\rm e}$ values.

3. Giant shells in the LMC

Giant shells are common in the LMC. They are generated by the combined action of stellar winds and supernova explosions originating from OB associations. The interiors are usually hot and low density and are often surrounded by a dense shell of optically radiating gas. The properties of giant shells will vary between examples but they typically expand with velocities of a few tens of kilometres per second and have radii of up to 100 parsecs (Meaburn 1988). The thickness of the dense shell wall is about a few parsecs (Oey 1996). McCray & Kafatos (1987) point out that the LMC is a particularly conducive environment for giant shell formation. The average ambient density is low, which allows rapid growth in shell size; the vertical scale-height is large, which reduces the tendency of shells to 'blow out'; and the metallicity is low, which thus reduces radiative losses somewhat.

Table 1. The local density ratios for some velocity spikes and the ambient medium. Column 1: the velocity features in Figs. 2a–d are identified either for a spike or the background ambient gas. Column 2: the $V_{\rm HEL}$ range for the density measured is indicated. Column 3: the measured [S II] 6716 Å/6731 Å intensity ratios. Column 4: the derived local electron densities.

Spike	$V_{\rm HEL}$ range km s^{-1}	[S II] 6716 Å/6731 Å	N_e $T_{\rm eff} = 10^4$K
A	106–230	1.19 ± 0.02	251 ± 30
B	94–218	1.11 ± 0.02	371 ± 25
C	87–199	1.16 ± 0.02	293 ± 30
D	68–220	1.07 ± 0.02	432 ± 30
E	64–184	1.10 ± 0.02	387 ± 30
F	136–223	1.27 ± 0.02	160 ± 20
Ambient			
G	248–273	1.45 ± 0.03	< 26
H	248–273	1.35 ± 0.03	89 ± 20

3.1. Shell instabilities

Old supernova generated shell walls are prone to instabilities. Many such shells appear incomplete or irregular at optical wavelengths while the X-ray interiors are often spherically symmetric. Hester (1987) argues that this is due to the variations in the external ambient medium density. Portions of the remnant encountering dense gas cool quickly and emit more optical photons than those portions advancing into a lower density environment. Hester (1987) also describes how the bumpy irregular nature of such shells will give rise to the filamentary nature of older SNR due to projection effects. Alternatively, Mac Low & Norman (1993) invoke dynamical overstabilities in blast waves to generate the optical detailed structure of SNR.

The Rayleigh-Taylor (R-T) instability is not expected to develop at this stage because a shell of gas expanding into the interstellar medium will decelerate due to the pick-up of stationary gas. If however the external density distribution drops off more rapidly than an inverse square law, the shell will accelerate. This will generate a R-T instability due to the presence of hot gas underlying cold gas in an effective gravitational field.

The tendency of cool dense shells to fragment into a collection of clumps via one of the instabilities described above may be curtailed somewhat if hot gas flows through breaks in the shell but ablates colder gas. In this case, Meaburn et al. (1988) argue that the shell might reseal, resulting in a blister structure at the edge of the remnant. This suggestion is supported by their detection in velocity data of such a blister in the Vela supernova remnant (Meaburn et al. 1988).

4. Model

We assume that a supernova explosion takes place close to the wall of an old giant shell that, we further assume, has already begun to slowly fragment due to the R-T instability but has not yet fragmented into a collection of individual clumps (see Meaburn et al. 1988).

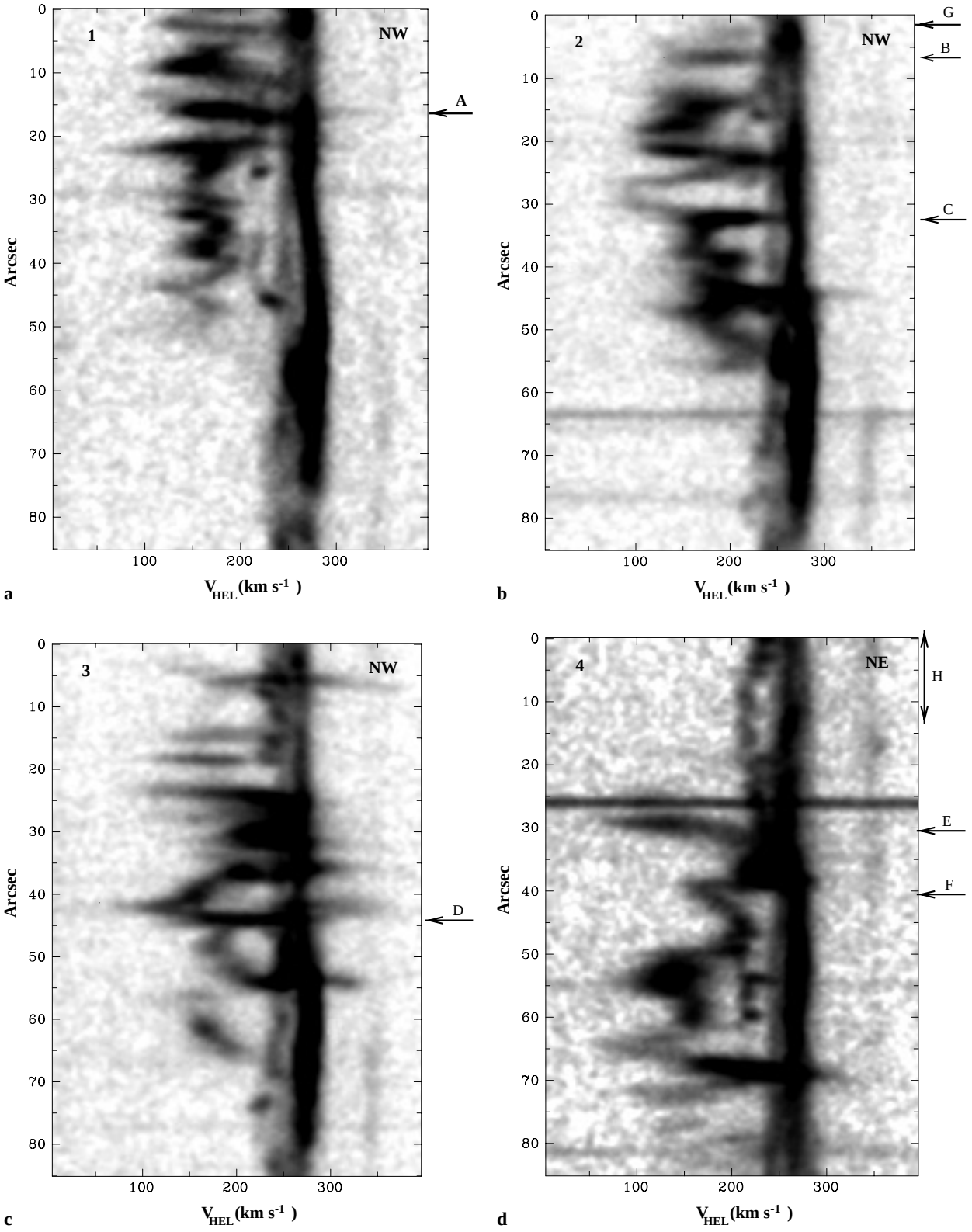

Fig. 2a–d. Negative, greyscale representations of the position–velocity arrays of [S II] 6716 & 6731 Å profiles from parts of the slit positions 1–4 are shown in a–d respectively. The velocity features A–H whose local electron densities have been tabulated in Table 1 are indicated

This latter assumption is supported by CO observations of the LMC obtained by Cohen et al. (1988). The 30 Doradus region is located near the tip of an elongated region of molecular gas. SN 1987a, which is located close to the Honeycomb nebula

is found towards the edge of this molecular material. It is thus possible that the shell is expanding into an environment in which the ISM density drops rapidly with distance, triggering the RT instability as described in Sect. 3.

The former assumption is plausible since a giant shell will take $\lesssim 10^7$ yrs to reach ~ 100 pc. With a velocity dispersion amongst cluster members of $\sim 10\ \mathrm{km\ s^{-1}}$, the OB association that initiated the shell growth will have dispersed over this time to occupy a similar sized volume. Note also that the OB association will have also lost its highest mass (and most luminous) members to supernovae explosions by this time so that it will be difficult to discern cluster members from field B stars (McCray & Kafatos 1987). The supernova is required to drive the high velocity flow through the old shell and illuminate the resulting Honeycomb structure.

The fastest growing wavelengths of the RT instability are those of order the shell thickness. The growth timescale, $t_{\rm g}$, is given by

$$t_{\rm g} \sim \left(\frac{\Delta}{\ddot{R}}\right)^{1/2} \sim \left(\frac{\Delta}{R}\right)^{1/2} t_{\rm D}, \tag{1}$$

where $t_{\rm D}$ is the dynamical age, $\ddot{R}$ is the acceleration and Δ is the thickness of the shell. Taking a shell of radius $R \sim 50$ pc with a thickness $\Delta \sim 1$pc(Oey 1996) gives $t_{\rm g} \sim t_{\rm D}/7$. The dynamical timescale, for an expansion velocity of $\simeq 50\,\mathrm{km\ s^{-1}}$, is $t_{\rm D} \sim R/\dot{R} \sim 10^6$ yr. The growth of the instabilities can result in the venting of the hot gas since the mass content per unit area in the shell will be at a minimum at points which are separated by distances of approximately Δ. The densities inferred from the [S II] ratios (Sect. 2) are consistent with the shell thickness and radius used above since if all swept up matter is in the shell, then

$$\frac{R}{\Delta} \simeq \frac{3N_{\rm s}}{N_{\rm a}} \tag{2}$$

where $N_{\rm s}$ is the shell density and $N_{\rm a}$ is the ambient medium density. Using our measured values of $N_{\rm s} \sim 350$ and $N_{\rm a} \sim 30$ (Sect. 2) gives $R/\Delta \sim 40$.

4.1. The generation of the Honeycomb nebula

We assume that after fragmentation of the giant shell, a supernova occurs within the shell interior; that the repressurization near these fragments is sufficient to drive a strong shock through them and that the shocked fragment gas cools quickly; finally that in the final fragment configuration, the magnetic pressure greatly exceeds the thermal pressure there. Hot interior gas will flow outwards past the fragments. We assume that this flow is supersonic and that the magnetic field is parallel to the boundary layer set up at the hot gas – fragment interface. In this boundary layer, momentum and energy is transferred to fragment gas which is accelerated outwards. We identify this material with the spike gas.

We follow the treatment of Dyson et al. (1995) and Malone (1996) to estimate the velocity of the accelerated gas. The basic assumptions are: (a) there is a bow shock of a specified shape between the supersonic hot gas and the boundary layer; (b) the component of the wind velocity perpendicular to the shock at any point in the shock is thermalized; (c) the tangential velocity component is conserved and injects momentum into the layer; (d) the ram pressure of the perpendicular component of the momentum flux is balanced by the magnetic pressure; (e) the boundary layer is isothermal at temperature T.

The velocity of the accelerated gas, $V_{\rm s}$ is then (Dyson et al. 1995, Malone 1996)

$$V_{\rm s} \simeq 2c_{\rm L}\left(\frac{d}{\delta}\right)^{1/2}\beta^{1/2} \tag{3}$$

where $c_{\rm L}$ is the sound speed in the boundary layer; d/δ is the ratio of the layer length to the layer thickness; β is the ratio of the magnetic pressure to the gas pressure in the clump. Hartquist & Dyson (1988) and Cantó & Raga (1991) estimate $d/\delta \simeq 10$–20. Taking $d/\delta = 10$ and $\beta = 10$ gives that $V_{\rm s} \simeq 20c_{\rm L}$. Hence for an estimated spike gas temperature of 10^4 K, $c_{\rm L} \simeq 10\ \mathrm{km\ s^{-1}}$ and so $V_{\rm s} \simeq 200\ \mathrm{km\ s^{-1}}$.

The measured velocity will steadily increase along the boundary layer from the systemic to $V_{\rm s}$, in agreement with the observations. The puzzling characteristic cut off in the velocity spikes is simply due to the fact that the velocity is scaled by the sound speed of $10\ \mathrm{km\ s^{-1}}$ and that there is a fairly weak dependence on geometry. The narrowness of the velocity spikes in the spatial direction and their location at the edges of the Honeycomb cells have a natural explanation when one considers that the boundary layer is being viewed along its length.

Chu et al. (1995) suggested that the magnitude of the velocity spikes seen in Meaburn et al. (1995) could be due to very hot gas escaping sonically through pores in a dense shell inclined at 45° to the line of sight. This was suggested because of the difference between the the hot gas sound speed (estimated to be $\simeq 565\ \mathrm{km\ s^{-1}}$ from x-ray data) and the velocity spikes which extend to over $150\ \mathrm{km\ s^{-1}}$ compared to the systemic speed. However, if the Honeycomb is inclined at 45°, the shapes of the honeycomb cells would be significantly distorted. Also the bright velocity spikes (Figs. 2a–d) suggest that the flows are aligned with the line of sight and are at a lower temperature of $T \sim 10^4$ K.

An important issue is whether the piercing of the shell will be curtailed by the self-sealing blister effect. Interestingly, in the velocity data, there appears to be some evidence for self-sealing blisters at several of the cells (eg. in Fig. 2b just above label C). It is likely local variations in the shell conditions, particularly of the magnetic field, dictate whether or not the hot gas will be prevented from escape. For the flow to self-seal and form a blister, the boundary layer would have to thicken to half the diameter of the cell. δ will thicken to this degree if the mixing layer has a length of about 5–10 Δ. In the context of this model, this is incompatible with the assumption that the thickness of the shell is comparable to the cell size. Furthermore, the contrast ratio between the cell wall and cell centre would be much less than seen in the images in Fig. 1. Perhaps self-sealing occurs when the magnetic pressure no longer dominates the gas pressure. Then the acceleration is much less (see Eq. 3) and the layer

may broaden out if the velocities generated are about equal to the sound speed.

Finally, some of the brightest (blue-shifted) velocity spikes have a fainter red-shifted counterpart. This is not easily accounted for by our simple model. However, they may simply be due to forward scattering of the boundary layer flow by dust in the old shell wall (since the flow will be red-shifted in the frame of the shell). Spectropolarimetric observations could test this suggestion.

5. Conclusions

In this paper we have examined the processes that may have led to the generation of the structure and dynamics of the Honeycomb nebula. Previous work established that in all probability, the Honeycomb was generated by the interaction of a young supernova blast wave with the wall of a pre-existing giant shell. In this work, the origin of the striking Honeycomb pattern of the nebula and the associated (equally dramatic) velocity features have been addressed. We conclude that, from simple arguements, the cellular structure is the result of the blast wave from the young supernova explosion piercing the R-T unstable wall of the giant shell. The typical cell size arises simply because the dominant mode in the RT instablity is the one with a wavelength of the order of the shell thickness. The required shell wall thicknesses of around a parsec are consistent with those seen in the LMC. We interpret the narrow blue shifted velocity spikes, shown in detail in this paper, as arising from the boundary layer between the hot supernova remnant gas and the colder dense gas that comprises the shell wall. Both the magnitude of the velocity shift along the spikes and the location of the spikes on the edges of the cells are understood as the viewing of these boundary layers from a face on perspective. This is illustrated schematically in Fig. 3.

At present, the Honeycomb nebula appears to be the only such structure of its kind. There may be a combination of reasons for this. Firstly, the venting of the hot gas interior and the mixing with the dense shell material cannot continue indefinitely. The cell walls of connecting cells will be eroded - this may be taking place in some of the more central cells (see Fig. 1). The face on viewing angle assumed here is fortuitous. If the system was inclined to the line of sight then the Honeycomb structure would be hard to discern. Finally, if the scenario we have described is largely correct then it requires the supernova explosion to have taken place before the giant shell fragmented completely (in which case it would have become a collection of outward moving, possibly gravitationally unstable, clumps). The RT instability must have already been instigated however, in order that the length scale of the cells be established.

Acknowledgements. The early theoretical parts of this work benefitted greatly from discussions with the late Franz Kahn. We also thank Wolfgang Steffen and John O'Connor for useful discussions. We would like to thank the staff at the AAT, who provided their usual excellent service during the observing run. The SuperCOSMOS unit at the ROE kindly provided the image in Fig. 1a and coordinate information. MPR acknowledges support from PPARC through a Rolling Grant at Manchester. A King Abdulaziz City for Science and Technology 'KACST' studentship is acknowledged by ZAA. We thank the referee, Lister Staveley-Smith, for several helpful comments.

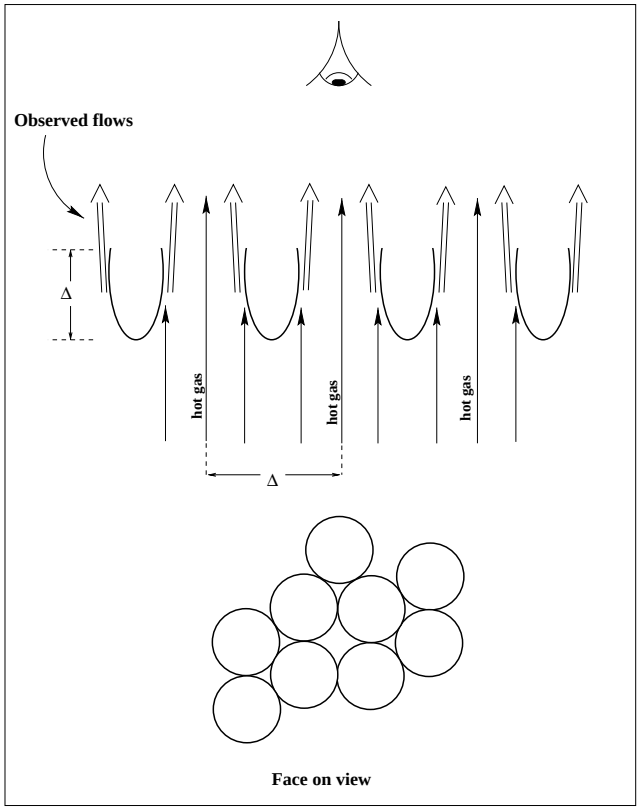

Fig. 3. A schematic diagram of the model of the Honeycomb nebula. The magnetic field is aligned parallel to the boundary layer flow (double lines). This flow at the edge of the Honeycomb cells is identified with the velocity spikes seen in Fig. 2

References

Cantó J., Raga A.C., 1991, ApJ 372, 646
Chu Y.-H., Dickel J.R., Staveley-Smith L., Osterberg J., Smith R.C., 1995, AJ 109, 1729
Cohen R.S., Dame T.M., Garay G., et al., 1988, ApJ 331, L95
Dyson J.E., Hartquist T.W., Malone M.T., Taylor S.D., 1995, Rev. Mex. Astron. Astrofis. Series de Conferencias 1, 29
Hartquist T.W., Dyson J.E., 1988, Ap&SS 144, 615
Hester J.J., 1987, ApJ 314, 187
Mac Low M.M., Norman M.L., 1993, ApJ 407, 207
Malone M.T., 1996, Ph.D. Thesis, Victoria Univ. Manchester
McCray R., Kafatos M., 1987, ApJ 317, 190
Meaburn J., 1988, MNRAS 235, 375
Meaburn J., 1991, In: Haynes R., Milne D. (eds.) IAU Symposium 148: The Magellanic Clouds. p. 421
Meaburn J., Blundell B., Carling R., et al., 1984, MNRAS 210, 463
Meaburn J., Dyson J.E., Hartquist T.W., 1998, MNRAS 230, 243
Meaburn J., Laspias V., Solomos N., Goudis C., 1989, A&A 223, 497
Meaburn J., Wang L., Palmer J., López J.A., 1993, MNRAS 263, L6
Meaburn J., Wang L., Bryce M., 1995, A&A 293, 532
Oey M.S., 1996, ApJ 467, 666
Saraph H.E., Seaton M.J., 1979, MNRAS 148, 367
Walborn N. R., Barbá R. H., Brandner W., et al., 1999, AJ 117, 225
Wang L., 1992, ESO Messenger 69, 34